Bends and splitters for self-collimated beams in photonic crystals

Xiaofang Yu
Department of Applied Physics, Stanford University, Stanford, California 94305

Shanhui Fan[a)]
Department of Electrical Engineering, Stanford University, Stanford, California 94305

(Received 28 July 2003; accepted 27 August 2003)

We present finite-difference time-domain studies for self-collimated beams in photonic crystal structures. Using a pulse propagation technique that eliminates the interference from the boundary of finite photonic crystal structures, we show that the self-collimation phenomena can occur within a relatively wide bandwidth. We also demonstrate near-perfect operation efficiencies over wide frequency ranges in bends and splitters constructed by simply truncating the photonic crystal. © *2003 American Institute of Physics.* [DOI: 10.1063/1.1621736]

The complex spatial dispersion properties in photonic crystal (PC) structures provide mechanisms to control the flow of light.[1–10] Of particular interest is the self-collimation effect,[3,6–10] by which a beam of electromagnetic wave can propagate with almost no diffraction in a perfectly periodic PC. Recent works in two-dimensional PC structures[6–10] have demonstrated such an effect as an on-chip wave-guiding mechanism. In this letter, we present a computational study of the bandwidth of the self-collimated phenomena using a pulse propagation technique that eliminates the interference from the reflection at the boundary of finite PC structures. We also demonstrate near-perfect operation efficiencies over wide frequency ranges in bends[10] and splitters constructed by simply truncating the PC. Our works provide further evidence of the intriguing potentials of self-collimated beams as a basis for on-chip integrated photonic circuits.

We choose to study a crystal shown in the inset of Fig. 1, which consists of a square lattice of air holes introduced into a high index material ($\varepsilon=12$). The holes have a radius of $0.35a$, where a is the lattice constant. As can be seen in Fig. 1 in the constant-frequency contour representation of the band diagram for the TE modes,[4,5] (the TE modes have the electric field perpendicular to the axis of the air holes), such a crystal provides wide-angle self-collimated propagation along the [11] direction for the frequencies in the vicinity of $f=0.19(c/a)$.

To quantify the diffraction behaviors of self-collimated beams, we truncate the crystal at a (11) surface, and place an external dielectric waveguide, with a width of $5a$, perpendicular to such surface [Fig. 2(a), inset]. A pulse consisting of the fundamental mode of the waveguide is then excited and incident upon the crystal. We monitor the propagation properties of the beam thus generated inside the crystal, by recording the magnetic-field amplitudes at the center of the beam at several monitor points. The field amplitude as a function of time steps taken at one such monitor point is shown in Fig. 2(a). The field amplitude consists of a forward-propagating initial pulse that is generated by the externally incident light, and a back-reflected pulse from the boundary of the crystal at the far end. With the use of a sufficiently large crystal ($23\sqrt{2}a\times 98\sqrt{2}a$), these two pulses become temporally separated. The Fourier transformation of only the initial pulse thus yields the propagation properties of an optical beam inside a crystal, without the artifacts introduced by the reflections at the crystal boundaries.

Using such a technique, we study the normalized intensity spectra for the forward-propagating initial pulse in the crystal, at several monitor points located at distances ranging from $8.5\sqrt{2}a$ to $58.5\sqrt{2}a$ away from the truncation of the crystal [Fig. 3(b)]. The normalization is obtained with respect to the intensity spectrum for a monitor point located at $3.5\sqrt{2}a$ from the (11) interface. In most frequency regions, the intensity decreases rapidly as a function of propagation distance, indicating the presence of strong diffraction. We note, however, a frequency range between 0.186 and $0.192c/a$, in which the intensity at the center of the beam remains above 85% over a propagation distance of $55\sqrt{2}a$, for a beam width of approximately $5a$. (In comparison, the intensity at the center of a beam excited by the same dielec-

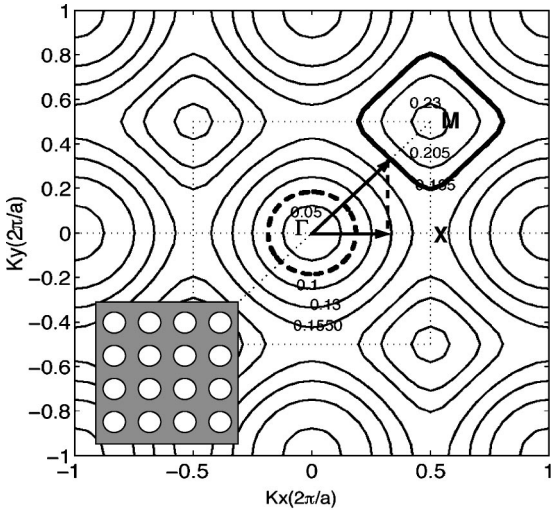

FIG. 1. Equal frequency contour for a PC structure. The PC structure, which consists of square lattice of air holes introduced in dielectric ($\varepsilon=12$), is shown in the inset. The thick solid line indicates the contour at $f=0.185(c/a)$ in the vicinity of which the self-collimation effects occur. The thick dashed lines are the equal frequency contour for air at $f=0.185(c/a)$.

[a)]Electronic mail: shanhui@stanford.edu

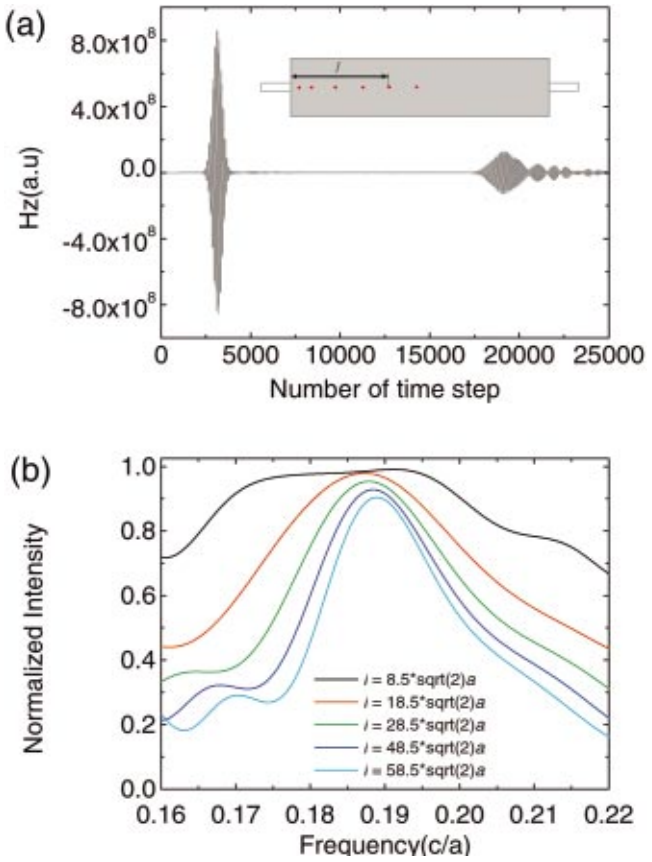

FIG. 2. (Color) (a) The inset shows the schematic of the computational domain used for the study of self-collimation phenomena. The gray region is the PC region. The crystal is truncated at a (11) surface through the center of the air holes. A dielectric waveguide represents by the rectangle excites a beam inside the PC. The red dots represent the monitor points inside the crystal. These monitor points are located at the center of the beam. The figure shows the magnetic field as a function of time step at a monitor point. Notice the temporal separation of the initial propagating pulse, and the reflected pulse from the far end of the crystal. (b) Intensity spectra at the monitor points, as shown in (a), at distances of $8.5\sqrt{2}a$, $18.5\sqrt{2}a$, $28.5\sqrt{2}a$, $48.5\sqrt{2}a$, and $58.5\sqrt{2}a$ away from the crystal boundary. The spectra are normalized with respect to the magnetic-field spectrum recorded at the monitor point located at $3.5\sqrt{2}a$ from the crystal boundary.

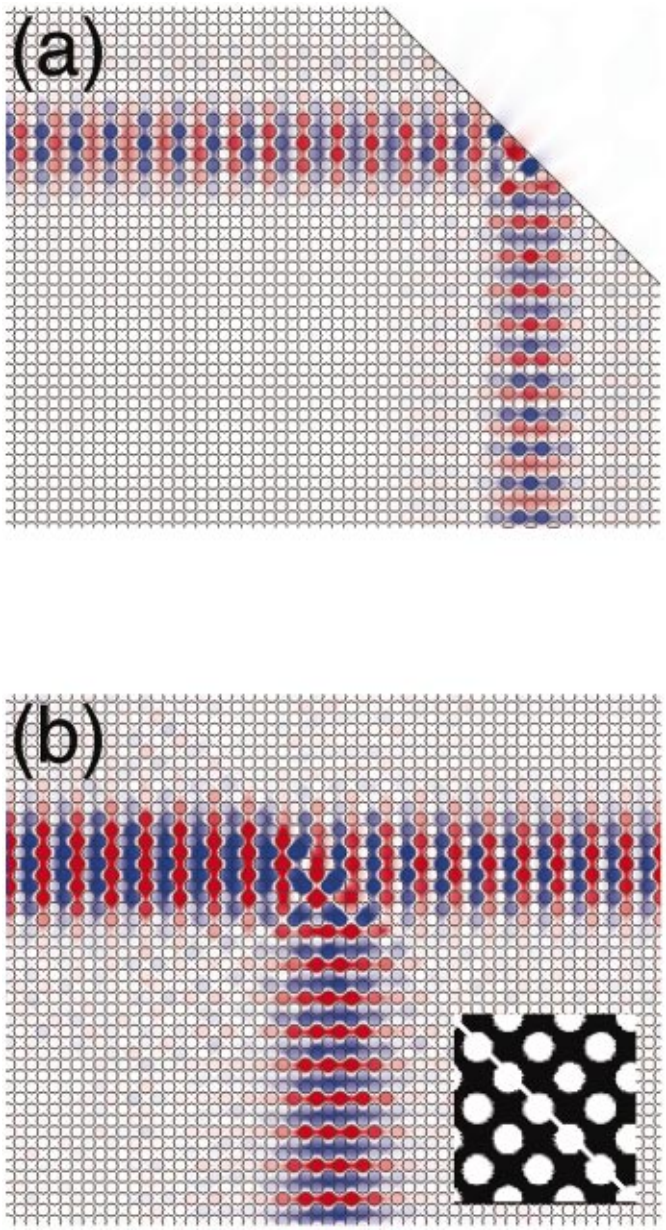

FIG. 3. (Color) Magnetic-field distribution as a self-collimated beam propagates through (a) bend and (b) splitter geometry. Red and blue represent large positive and negative amplitudes, respectively. The solid lines indicate the position of the air holes. The inset in (b) shows the magnified version of the structure in the vicinity of the air trench at which the beam splitting occurs.

tric waveguide and propagates in a uniform Si region would have dropped to approximately 20% over the same propagation distance.) This frequency range corresponds well with the self-collimation region in the band structure calculation shown in Fig. 1, and represents a bandwidth of approximately 50 nm when the operating wavelength is in the vicinity of 1.55 μm. Thus, even with a beam that possesses a relatively small cross section, the self-collimation phenomenon should in fact possess sufficient bandwidth to function as an effective waveguide mechanism through a substantial propagating distance.

In order for self-collimated beams to function as a basis for integrated photonic circuits, it is also important to provide a mechanism for bends and splitters. In examining the constant frequency diagram shown in Fig. 1, we note that the wave vector region where the self-collimation occurs has a k_x value that lies outside the constant frequency contour for air. Therefore, a (10) crystal–air interface should behave as a total internal reflection mirror for self-collimated beams propagating along the [11] direction, and can be used to create a sharp 90° bend[10] [Fig. 3(a)]. Moreover, a beam splitter can be designed by bringing two of such (10) crystal–air interfaces in close proximity to each other [Fig. 3(b)], with the distance between the two interfaces controlling the power-splitting ratio [Fig. 3(b)].

To quantify the efficiency of such bends or splitters, we again employ a large enough crystal ($23\sqrt{2}a \times 48\sqrt{2}a$ for bend, and $98\sqrt{2}a \times 98\sqrt{2}a$ for splitter) such that the results are free from the reflected pulse from the crystal boundaries (Fig. 4, insets). The same dielectric waveguide as shown in Fig. 2 is used to generate a beam propagating in the [11] direction. Such a beam is then incident upon the (10) crystal–air interfaces and is either bent or split. We integrate the intensity across the beam cross section in order to obtain the power in the incident, bent, or transmitted beam, and we obtain the efficiency of the bend or the splitter by normalizing with respect to the incident power.

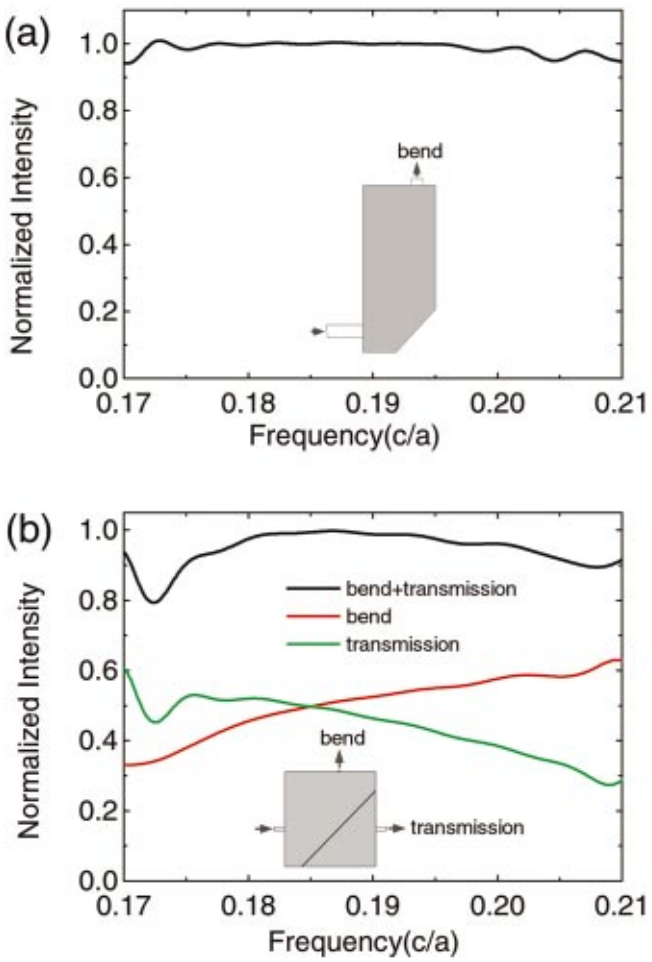

FIG. 4. (Color) (a) Bending efficiency for the 90° bend shown in Fig. 3(a). (b) The red and green lines are the bending and transmission efficiency for the splitter shown in Fig. 3(b); the black line represents the sum of the bending and transmission efficiency. The insets in both (a) and (b) are a schematic of the computational setup. The gray region represents the PC, and the white rectangular represent the dielectric waveguide used to excite the beam.

In the case of a single interface [Fig. 3(a)], the bending efficiency is shown in Fig. 4(a). Near 100% bending efficiency is accomplished over the entire frequency bandwidth within which self-collimation occurs. In the case of a splitter, where two interfaces are present [Fig. 3(b)], the power spectra in the transmitted or bent beam are shown in Fig. 4(b). Within the frequency range of self-collimation, the sum of the transmitted and bent power reaches near 100% over the entire self-collimation bandwidth. In addition, the structure behaves as a 50-50 splitter in the frequency range near $0.185c/a$ when the distance between the interfaces is $0.1a$. Importantly, no back reflection occurs in either the bend or the splitter. The steady field patterns at $f=0.19c/a$ for the bend and splitter are also shown in Fig. 3. We note that the beam profile is substantially unaltered through the interaction process.

As concluding remarks, unlike typical PC waveguides,[11,12] no detailed structure tuning is needed in order to suppress back reflection for self-collimated beams in a bend or splitter. The efficiency is near perfect over the entire wavelength range within which the self-collimation occurs. Moreover, while the simulations are two-dimensional, it has been shown in Ref. 6 that such a two-dimensional model in fact provides a good approximation to a three-dimensional PC slab structure. Therefore, our results strongly suggest the possibility of a completely different class of on-chip integrated photonic components based upon self-collimation phenomena.

This work was funded in part by the National Science Foundation (NSF) grant No. ECS-0200445, by Agilent Technologies through the Center for Integrated Systems (CIS) at Stanford University, and by a 3M untenured faculty award. The simulations were performed through the support of a NSF-NRAC program.

[1] S.-Y. Lin, V. M. Hietala, W. Li, and E. D. Jones, Opt. Lett. **21**, 1771 (1996).
[2] H. Kosaka, T. Kawashima, A. Tomita, M. Notomi, T. Tamamura, T. Sato, and S. Kawakami, Phys. Rev. B **58**, R10096 (1998).
[3] H. Kosaka, T. Kawashima, A. Tomita, M. Notomi, T. Tamamura, T. Sato, and S. Kawakami, Appl. Phys. Lett. **74**, 1212 (1999).
[4] M. Notomi, Phys. Rev. B **62**, 10696 (2000).
[5] C. Luo, S. G. Johnson, J. D. Joannopoulos, and J. B. Pendry, Phys. Rev. B **65**, 201104 (2002).
[6] J. Witzens, M. Loncar, and A. Scherer, IEEE J. Sel. Top. Quantum Electron. **8**, 1246 (2002).
[7] D. N. Chigrin, S. Enoch, C. M. Sotomayor Torres, and G. Tayeb, Opt. Express **11**, 1203 (2003).
[8] J. Wiltzens and A. Scherer, J. Opt. Soc. Am. A **20**, 935 (2003).
[9] L. Wu, M. Mazilu, and T. F. Krauss, J. Lightwave Technol. **21**, 561 (2003).
[10] C. Chen, A. Sharkawy, S. Shi, and D. W. Prather, *Integrated Photonics Research, OSA Technical Digest* (Optical Society of America, Washington DC, 2003), p-39.
[11] A. Mekis, J. C. Chen, I. Kurland, S. Fan, P. R. Villeneuve, and J. D. Joannopoulos, Phys. Rev. Lett. **77**, 3787 (1996).
[12] S. Fan, S. G. Johnson, J. D. Joannopoulos, C. Manolatou, and H. A. Haus, J. Opt. Soc. Am. B **18**, 162 (2001).